

## Design of a fiber optical sensor for atmospheric electric field measurement

H.V. Baghdasaryan<sup>1</sup>, A.V. Daryan<sup>2</sup>, T.M. Knyazyan<sup>1</sup>

1. Fiber Optics Communication Laboratory, National Polytechnic University of Armenia, 105 Terian str., Yerevan 0009, Armenia;

2. A.Alikhanyan National Lab (Yerevan Physics Institute), 2, Alikhanyan Brothers, Yerevan 0036, Armenia

**Abstract.** All-optical sensor for atmospheric electric field detection and measurement is suggested and numerically modelled. Thin electro-optical crystal sandwiched between two distributed Bragg reflectors (DBRs) forming multilayer Gires-Tournois (G-T) microresonator is used as a sensitive part of the electric field sensor. In the sensor device, an optical fiber delivers the wideband light spectrum to the sensing multilayer structure of G-T microresonator. The reflectance spectrum of the sensor contains information on the electric field strength and direction. The relevant reflectance peaks' shift in the reflected spectrum can be observed by an optical spectrum analyzer (OSA). Numerical modelling has been done by the method of single expression that is a suitable tool for multi-boundary problems solution. The obtained results of modelling will be useful in a new type of non-distorting sensor's elaboration for atmospheric electric field detection and measurement.

### 1. INTRODUCTION

The magnitude of atmospheric electric field is an important parameter in evaluation of the atmosphere state [1-3]. Measurements of the atmospheric electric field provide information about the thunderstorm activity and are useful for weather forecasting and lightning alert. Conventional instrument used for measuring the strength of electric fields in the atmosphere near thunderstorm clouds is the "field mill" [4, 5]. Different types of "field mills" and E-field probes for electric field measurement and relevant devices are under exploitation [4-9]. However, all these devices are prepared by or contain metallic parts and wires, which distort the electric field distribution [10, 11]. Use of electro-optical sensors makes possible creation of metallic free electric field meters. Devices of this type are widely used in high voltage (HV) engineering, antenna and electromagnetic compatibility (EMC) measurements, etc. [9, 12-14].

Photonic field meters utilize the Pockels effect or linear electro-optic (EO) effect, which produces birefringence in an optical medium. Substances such as KDP (Potassium Dihydrogen Phosphate), KD\*P (Deuterated KDP) and LiNbO<sub>3</sub> (Lithium Niobate) show large Pockels effect and are very popular in electro-optic modulators [15].

Electric field measurement by use of the Pockels effect implies some means of measuring a change in refractive index caused by the applied electric field. Change in refractive index causes phase change of light passing through the EO crystal. Therefore, the problem reduces to the determination of the phase shift. There are devices exploiting direct measuring of phase shift by means of non-resonant interference methods [13, 16, 17].

We consider another type of electro-optical sensors using nonlinear resonator. These sensors contain an optical fiber and electro-optical crystal within micro-resonator mounted on the end of the fiber [10, 11, 13, 18-20]. Change in the refractive index induced by an external electric field causes shift of the reflectance spectrum. Resonator is irradiated by a wideband optical source via optical fiber and optical spectrum analyzer is used for detection of the reflected light. The same configuration can operate by using monochromatic light source performing phase shift measurement. In this case, phase shift is more sensitive than that in non-resonant case.

The wide range of atmosphere electric field's variation complicates the operation of electro-optical sensor and requires thorough computer simulations before specific device realization. In this paper the relevant method for simulation of light propagation and reflection in the proposed optical design is presented.

### 2. CONSTRUCTION AND MEASUREMENT SCHEME OF ELECTRO-OPTICAL SENSOR

For measurement of atmospheric electricity the following construction of all-optical sensor is suggested (Fig.1.):

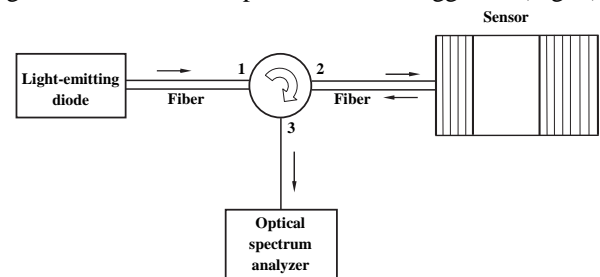


Figure 1. All-optical sensor for atmospheric electric field measurement.

A wideband optical source (light-emitting diode) illuminates reflective microresonator and the spectrum of reflected light is observed by optical spectrum analyzer (OSA). The sensor is a reflective type of Fabry-Perot microresonator (Gires-Tournois (G-T) [21]) where electro-optical crystal is sandwiched between DBR mirrors (Fig. 2).

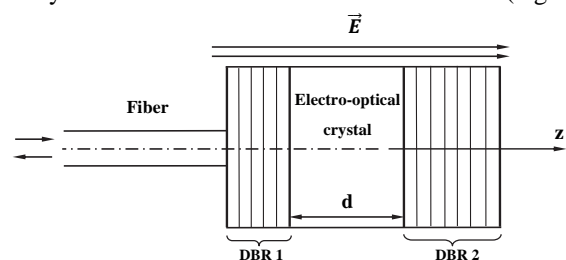


Figure 2. All-optical sensor consists of optical fiber and Gires-Tournois microresonator formed by electro-optical crystal sandwiched between two DBR mirrors of high (DBR 2) and medium reflectivity (DBR 1).

The z-cut electro-optical crystal is sensitive to the electric field strength  $\vec{E}$  directed parallel or anti-parallel to the z-axis. Let us consider an application of electro-optical

crystal LiNbO<sub>3</sub> as a sensitive part of micro-resonator. It is known that the variation of the refractive index of LiNbO<sub>3</sub> crystal by the amplitude of applied electric field is expressed as:

$$\Delta n = n^3 r_{33} E / 2, \quad (1)$$

where  $n = \sqrt{\varepsilon}$  is the refractive index at the absence of external electric field,  $r_{33} \approx 30.8 \cdot 10^{-12}$  m/V is an electro-optic coefficient of the material [22]. The sign of the index change depends upon the polarity of the voltage applied to the crystal [15].

Atmospheric electric field is changed in the range of  $E = 10^2 - 10^5$  V/m and relevant interval of permittivity change by (1) is:  $\Delta \varepsilon = 0.79 \cdot 10^{-6} - 0.79 \cdot 10^{-3}$ . Here  $n = 2$  is taken at the light wavelength  $\lambda_0 = 1.55 \mu\text{m}$ .

Multilayer DBR mirrors are alternating quarter-wavelength bilayers of low and high permittivity providing high reflectance of mirrors necessary for microresonator operation. To determine optical characteristics of the microresonator the numerical simulation by means of the method of single expression (MSE) is carried out [23-28]. In the MSE, the solution of Helmholtz equation in each layer of the structure is searched in the form of a single expression, but not in the form of counter-propagating waves as in the traditional approach. Due to this, a prior assignment of the waveform in each layer of the structure is not required, which makes the MSE a convenient tool in studies of optical structures consisting of layers with any complex values of permittivity and permeability. The MSE is a valid tool for solving intensity-dependent non-linear problems since it does not rely on superposition principle.

### 3. CONCISE DESCRIPTION OF THE MSE

The backbone of the MSE for wave normal incidence on a multilayer structure is presented [23-28]. From Maxwell's equations in 1D case the following Helmholtz's equation can be obtained for linearly polarized complex electric field component  $\dot{E}_x(z)$ :

$$\frac{d^2 \dot{E}_x(z)}{dz^2} + k_0^2 \tilde{\varepsilon}(z) \dot{E}_x(z) = 0, \quad (2)$$

where  $k_0 = \omega / c$  is the free space propagation constant,  $\tilde{\varepsilon}(z) = \varepsilon'(z) + j\varepsilon''(z)$  is the complex permittivity of a medium. The essence of the MSE is presentation of a general solution of Helmholtz' equation for electric field component  $\dot{E}_x(z)$  in the special form of a single expression:

$$\dot{E}_x(z) = U(z) \cdot \exp(-jS(z)) \quad (3)$$

instead of traditional presentation as a sum of counter-propagating waves. Here  $U(z)$  and  $S(z)$  are real quantities describing the resulting electric field amplitude and phase, respectively. Time dependence  $\exp(j\omega t)$  is assumed but suppressed throughout the analysis. Solution in the form (3) prevails upon the traditional approach of counter-propagating waves and is more general because it is not relied on the superposition principle. This form of solution describes all possible distributions of electric field amplitude, corresponding to propagating or evanescent waves in a medium of positive or negative permittivity, respectively. No preliminary assumptions concerning the Helmholtz's equation solutions in different media are needed in the

MSE. This gives advantages in investigation of wave interaction with any longitudinally non-uniform linear and intensity dependent non-linear media that can be done with the same ease and exactness.

Based on expression (3) the Helmholtz's equation (2) is reformulated to the set of first order differential equations regarding the electric field amplitude  $U(z)$ , its spatial derivative  $Y(z)$  and a quantity  $P(z)$  - proportional to the power flow density (Poynting vector) in a medium:

$$\begin{cases} \frac{dU(z)}{d(k_0 z)} = Y(z) \\ \frac{dY(z)}{d(k_0 z)} = \frac{P^2(z)}{U^3(z)} - \varepsilon'(z) \cdot U(z) \\ \frac{dP(z)}{d(k_0 z)} = \varepsilon''(z) \cdot U^2(z) \end{cases} \quad (4)$$

where  $P(z) = U^2(z) \frac{dS(z)}{d(k_0 z)}$ . The sign of  $\varepsilon'(z)$  can take either

positive or negative describing relevant electromagnetic features of dielectric or metal (plasma), correspondingly. The sign of  $\varepsilon''(z)$  indicates loss or gain in a medium.

The set of differential equations (4) is integrated numerically starting from the non-illuminated side of a multilayer structure, where only one outgoing travelling wave is supposed. Initial values for integration are obtained from the boundary conditions of electrodynamics at the non-illuminated side of the structure. Numerical integration of the set (4) goes step by step towards the illuminated side of the structure taking into account an actual value of structure's permittivity for the given coordinate at each step of integration. In the process of integration any variable of the set (4) is possible to record in order to have full information regarding distributions of electric field amplitude, its derivative and power flow density inside and outside of the structure. At the borders between constituting layers of the multilayer structure ordinary boundary conditions of electrodynamics bring to the continuity of  $U(z)$ ,  $Y(z)$  and  $P(z)$ . From the boundary conditions of electrodynamics at the illuminated side of the structure the amplitude of incident field  $E_{inc}$  and the power reflection coefficient  $R$  are restored at the end of calculation. The power transmission coefficient  $T$  is obtained as the ratio of the transmitted power to the incident one.

### 4. NUMERICAL ANALYSIS OF A GIRES-TOURNOIS MICRORESONATOR WITH DBR MIRRORS AND LiNbO<sub>3</sub> LAYER AS A SPACER

The electromagnetic modelling of the G-T microresonator structure presented in Fig.2 is performed. Corresponding permittivity profile and distribution of optical wave's electric component along the structure are presented in Fig.3.

In Fig. 3, the thickness of the electro-optical layer between DBR mirrors is taken about  $5 \mu\text{m}$  for demonstration only. In the modelled structure, the thickness of the electro-optical crystal is taken as  $d = 200 \mu\text{m}$ . The character of internal field distribution in the microresonator at  $d = 200 \mu\text{m}$  looks like in Fig.3, only the increased number of field oscillations within the electro-optical crystal is observed. Highly reflective DBR mirror consists of 13 SiO<sub>2</sub>/N-LASF9 bilayers and the front mirror consists of 7 bilayers.

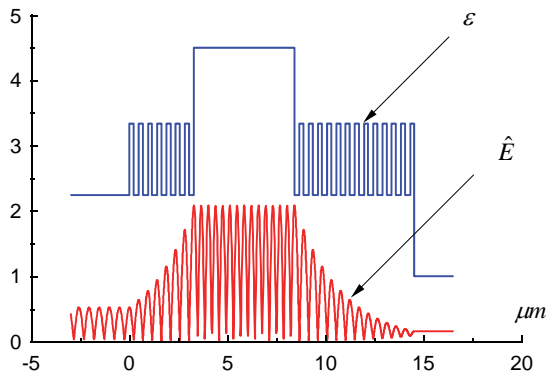


Figure 3. Permittivity profile  $\varepsilon$  and distribution of the amplitude of optical wave's electric field component  $\hat{E}$  along the G-T microresonator at the point of the lowest reflectance ( $R = 0.766$ ). Here the thickness of the electro-optical crystal is  $d = 5.115 \mu\text{m}$ , the layers of the mirrors are:  $L_{\text{SiO}_2} = 258 \text{ nm}$  of permittivity  $\varepsilon = 2.25$  and  $L_{\text{N-LASF}_9} = 212 \text{ nm}$  of permittivity  $\varepsilon = 3.34$  at  $\lambda_0 = 1.55 \mu\text{m}$ .

For detection of atmospheric electric field, the sensor's z-axis should be oriented along external field. To model electric field influence on spectral dependences relevant calculation has been done for unperturbed permittivity of the electro-optical crystal ( $\varepsilon = 4.5$ ) and at its change at the value  $\varepsilon = 4.505$ . This permittivity change is relevant to the change under the highest electric field amplitude. The results of calculations are presented in Fig.4.

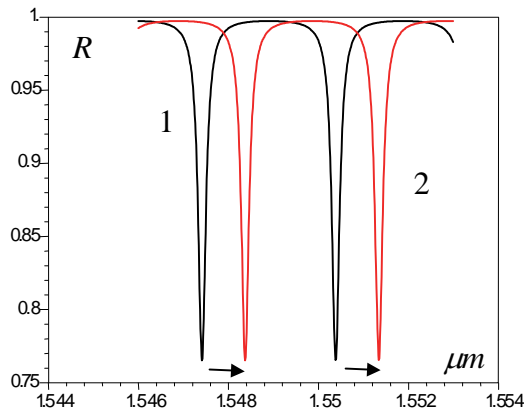


Figure 4. Spectral dependences of reflectance of microresonator (1) at unperturbed ( $\varepsilon = 4.5$ ) and (2) perturbed ( $\varepsilon = 4.505$ ) permittivity of electro-optical crystal. The right shift of spectral dependences stipulated by electrical field directed along crystal's z-axis.

At the change of external field direction, the permittivity of the crystal decreases and spectral peaks are shifted to the left.

The modelling permits to obtain information on the optimal multilayer mirrors suitable for the best observation of spectral peaks' shifts and information regarding influence of crystal thickness on the sensitivity of the sensor from the value of external electric field.

The obtained results will be useful in design and realization of all-optical atmospheric electric field detecting and measuring device. The directional sensitivity of the electro-optical crystal will permit to detect also the direction of atmospheric field that is also important in atmospheric field monitoring.

#### ACKNOWLEDGEMENTS

The authors are thankful to the participants of International Conference TEPA-2015 for fruitful discussions.

#### REFERENCES

- [1] X. Qiea et al. The possible charge structure of thunderstorm and lightning discharges in northeastern verge of Qinghai-Tibetan Plateau. *Atmospheric Research*, **76** (2005), pp. 231-246.
- [2] M. J. Rycroft et al. An Overview of Earth's Global Electric Circuit and Atmospheric Conductivity. *Space Sci. Rev.*, **137** (2008), pp. 83-105.
- [3] A.J. Bennett<sup>1</sup>, R.G. Harrison. Variability in surface atmospheric electric field measurements. *Journal of Physics: Conference Series*, **142** (2008), 012046.
- [4] J. Montanya` et al. A new electrostatic field measurement method: The coherent-notch field mill, *Journal of Electrostatics*, **65** (2007), pp. 431-437.
- [5] P. Tant, Design and Application of a Field Mill as a High-Voltage DC Meter, *IEEE Trans. Instrument. Measur.* **56** (2007), pp. 1459-1464.
- [6] A. Fort, Design, Modeling, and Test of a System for Atmospheric Electric Field Measurement, *IEEE Trans. Instrum. Measur.* **60** (2011), pp. 2778-2785.
- [7] N. A. F. Jaeger, *Integrated-Optic Sensors for High-Voltage Substation Applications*, SPIE **3489** (1998), pp. 41-52.
- [8] Hong-Sik Jung, Electro-optic Electric Field Sensor Utilizing Ti: LiNbO<sub>3</sub> Symmetric Mach-Zehnder Interferometers, *Journal of the Optical Society of Korea*, **16** (2012), pp. 47-52.
- [9] R. Zeng et al. Design and Application of an Integrated Electro-optic Sensor for Intensive Electric Field Measurement, *IEEE Trans. Dielectr. Electr. Insulat.*, **18** (2011), pp. 312-319.
- [10] Dong-Joon Lee et al. Recent Advances in the Design of Electro-Optic Sensors for Minimally Destructive Microwave Field Probing. *Sensors*, **11** (2011), pp. 806-824.
- [11] V.M.N. Passaro et al. Review: Electromagnetic field photonic sensors. *Progress in Quantum Electronics*, **30** (2006), pp. 45-73.
- [12] R.C.S.B.Allil, M.M. Werneck. Optical High-Voltage Sensor Based on Fiber Bragg Grating and PZT Piezoelectric Ceramics. *IEEE Trans. Instrument. Measur.*, **60** (2011), pp. 2118-2125.
- [13] H. Togo et al. Optical Fiber Electric Field Sensor for Antenna Measurement. *NTT Technical Review*, **7** (2009), pp.1-6.
- [14] M. Miki et al. Electric fields near triggered lightning channels measured with Pockels sensors. *Journal Geophys. Resear.* **107** (2002), pp. 1-11.
- [15] H. Nishihara, M. Haruna, T. Suhara. *Optical Integrated Circuits*. McGraw-Hill Book Company, 1989.

- [16] R. Forber et al. Dielectric EM Field Probes for HPM Test & Evaluation. Annual ITEA Technology Review, August 7-10, Cambridge, MA. Non-Intrusive Instrument. Technol. (2006), pp. 1-6.
- [17] F. Pan et al. An Optical AC Voltage Sensor Based on the Transverse Pockels Effect. Sensors, **11** (2011), pp. 6593-6602.
- [18] S.M. Chandani, Fiber-Based Probe for Electrooptic Sampling, IEEE PHOTON. TECHNOL. LETTERS, **18** (2006), pp.1290-1292.
- [19] Sh. Wakana et al., Fiber-Edge Electrooptic/Magneto-optic Probe for Spectral-Domain Analysis of Electromagnetic Field, IEEE Trans. Microwave Theory and Technol. **48** (2000), pp. 2611-2616.
- [20] K. Yang et al., Electric Field Mapping System Using an Optical-Fiber-Based Electrooptic Probe, IEEE Microwave Wireless Component. Lett. **11** (2001), pp. 164-166.
- [21] F. Gires, and P. Tournois. Interferometre utilisable pour la compression d'impulsions lumineuses modulees en frequence. C. R. Acad. Sci. Paris, **258** (1964), pp. 6112-6115.
- [22] D. A. Cohen et al. High-Q Microphotonic electro-optic modulator, Solids-State Electron., **45** (2001), pp. 1577-1589.
- [23] H.V. Baghdasaryan, A.V.Daryan, T.M. Knyazyan, K.U. Nikolaos. Modelling of non-linear enhanced performance Fabry-Perot interferometer filter, Microwave and Optical Technology Letters, **14** (1997), pp.105-108.
- [24] H.V. Baghdasaryan, Method of backward calculation, in the book: Photonic Devices for Telecommunications: how to model and measure/ Editor G.Guekos, Springer-Verlag, (1999), pp.56-65.
- [25] H.V. Baghdasaryan, T.M. Knyazyan, Problem of Plane EM Wave Self-action in Multilayer Structure: an Exact Solution, Optical and Quantum Electronics, **31** (1999), pp.1059-1072.
- [26] H.V. Baghdasaryan, T.M. Knyazyan, S.S. Berberyan, A.A. Mankulov, Correct Analysis of Gires-Tournois Absorbing Interferometer by the Method of Single Expression, Microwave and Optical Technology Letters, **37** (2003), pp. 64-67.
- [27] H.V. Baghdasaryan, T.M. Knyazyan, T.H. Baghdasaryan, B. Witzigmann, and F. Roemer, Absorption loss influence on optical characteristics of multilayer distributed Bragg reflector: wavelength-scale analysis by the method of single expression, Opto-Electronics Review, **18** (2010), pp. 438-445.
- [28] H.V. Baghdasaryan, Basics of the Method of Single Expression: New Approach for Solving Boundary Problems in Classical Electrodynamics. Monograph: Chartaraget, Yerevan, (2013), 164 pages.